Event-triggered Control for Discrete-time Saturated LPV Systems using a Partially-dependent Dynamic Output Controller ⋆

Carla de Souza * **Valter J. S. Leite** ** **Eugênio B. Castelan** ***

* *LAAS-CNRS, Toulouse, France. (e-mail: carla.souza93@hotmail.com).*
** *Department of Mechatronics Engineering, CEFET–MG, Divinópolis, MG. (e-mail: valter@ieee.org)*
*** *Department of Automation and Systems Engineering, DAS/CTC/UFSC, Florianópolis, SC. (e-mail: eugenio.castelan@ufsc.br).*

Abstract: In this paper, we propose an event-triggered control strategy based on a dynamic output-feedback controller for stabilizing discrete-time linear parameter-varying (LPV) systems. Such a controller has an anti-windup term and is partially dependent on time-varying parameters. To economize the limited network resources, two event generators are introduced on the sensor-to-controller and controller-to-actuator channels. They decide whether the current output measurement and control input should be sent through the network or not. Sufficient conditions in terms of linear matrix inequalities (LMIs) are provided to ensure the regional asymptotic stability of the closed-loop system and estimate its domain of attraction. The transmission activity is indirectly reduced thanks to appropriate optimization procedures. A numerical example testifies the efficiency of the proposed methodology.

Keywords: Event-based control. Systems with saturation. Linear parameter-varying systems. Output feedback control. Lyapunov methods.

1. INTRODUCTION

In recent years, the event-triggered control (ETC) has gained increasing attention due to its potential to reduce the communication burden and save network resources when compared to traditional periodic control (Tabuada, 2007). Contrasting with the latter, the event-triggering strategy operates in an aperiodic way. The control tasks are executed once a well-designed event condition is satisfied. In (Wu et al., 2014), the controller updates its value when the state-based error is higher than the state norm. However, for many control systems, the full state measurement is not always accessible. In theses cases, the design of output-based approaches become useful. Also, an important issue for ETC approaches is to find a larger enough minimum inter-event time avoiding the Zeno behavior (Girard, 2014), which is always guaranteed when dealing with discrete-time system. Several ETC techniques have been reported in the literature (see, for instance, (Heemels et al., 2012; Abdelrahim et al., 2015; Shen et al., 2019)). However, most of them handle only linear time-invariant (LTI) and non-linear systems.

Linear parameter-varying (LPV) systems represents a class of linear systems whose dynamics depends on online measurable time-varying parameters (Shamma, 2012). Although several control techniques have been proposed in the literature for such system (see, for instance, (Caigny et al., 2012; Briat, 2021)), only a few employ event-triggering mechanisms (ETMs). An event-triggered and self-triggered $\mathcal{H}_\infty$ output tracking control is established in (Huang et al., 2020) for discrete-time LPV systems with network-induced delays. A co-design condition in a sense of input- to-state practically stable (ISpS) of a mixed ETM and a static output-feedback controller is established in (Xie et al., 2018) for stabilization of discrete-time LPV systems. Golabi et al. (2016, 2017) address an event-based reference tracking control for discrete-time LPV systems by simultaneously designing event-triggering conditions and a state feedback controller. Braga et al. (2015) examine the problem of discretization and digital state/output feedback control design for continuous-time LPV systems subject to a time-varying networked-induced delay.

When it comes to practical control systems, an important aspect to consider is the presence of saturating actuators. As the closed-loop becomes non-linear, the regional stability must be managed, which requires the estimation of a region of attraction (Tarbouriech et al., 2011). In this context, Ding et al. (2020) propose an event-triggered control based on a static and a dynamic state feedback controller for discrete-time systems subject to actuator saturation. Zuo et al. (2016) provide a cone complementary linearization algorithm to solve a non-convex optimization problem in order to obtain the co-design of a state-feedback controller with saturation. A procedure to design

⋆ C. de Souza thanks ANR under the project HANDY number 18-CE40-0010. V. J. S. Leite and E. B. Castelan thanks the Brazilian Agency CNPq for the partial support (grants 311208/2019-3 and 306927/2017-9).

a static state feedback that maximizes an estimate of the domain of attraction of saturated discrete-time system for a given triggering function is investigated in (Wu et al., 2014).

In this paper, we address the problem of event-triggered control for discrete-time LPV systems subject to saturating actuators. Two event-triggering policies are introduced to reduce the data transmission of the output measurement and control input separately. Differently from de Souza et al. (2020), where a full parameter-dependent dynamic output-feedback controller (FPD-DOF) is designed to regionally stabilize the closed-loop system, here we employ a partially parameter-dependent (PPD-DOF) one. Consequently, simpler convex conditions are established, since there are fewer variables and matrix multiplications. Optimization procedures are also formulated allowing minimizing the transmission activity and, optionally, maximizing the estimate of the region of attraction at the same time. Through a numerical example, such aspects are used to compare the performance of both controller: PPD-DOF and the FPD-DOF.

Notation: $\mathbb{R}$ and $\mathbb{R}^+$ denote respectively the set of real and non-negative real numbers. $\mathbb{R}^{m\times n}$ is the set of matrices with real entries and dimensions $m \times n$. $\mathbf{0}$ and $\mathbf{I}_n$ stand respectively for the null matrix of appropriate dimensions and the identity matrix with dimensions $n \times n$. $A = \mathtt{diag}\{A_1, A_2\}$ is a diagonal matrix with block diagonal matrices A_1 and A_2. $\mathtt{tr}(A)$ denotes the trace of a square matrix A. $A_{(\ell)}$ indicates the ℓ^{th} line of a vector or a matrix A. $\mathcal{I}[a, b]$ denotes the set of integer numbers belonging to the interval from $a \in \mathbb{N}$ to $b \in \mathbb{N}$, $b \geq a$. The symbols $\star$ and $\bullet$ represent respectively the symmetric blocks within a matrix and an element that has no influence on development. For $x \in \mathbb{R}^n$, $\|x\| = \sqrt{x^\top x}$ denotes the Euclidean norm and $\|x\|_Q^2$ is defined by $x^\top Qx$ with $\mathbf{0} < Q = Q^\top \in \mathbb{R}^{n\times n}$.

2. PROBLEM STATEMENT

Consider the discrete-time system described by

$$\begin{aligned} x_{k+1} &= A(\vartheta_k)x_k + B(\vartheta_k)\mathtt{sat}(\hat{u}_k), \\ y_k &= Cx_k, \end{aligned} \tag{1}$$

where $x_k \in \mathbb{R}^n$ is the state vector, $\hat{u}_k \in \mathbb{R}^{n_u}$ is the most recently transmitted value of the control input $u_k \in \mathbb{R}^{n_u}$, and $y_k \in \mathbb{R}^{n_y}$ is the measurable output. The symmetric decentralized saturation function, $\mathtt{sat}(\hat{u}_k)$, is given by

$$\mathtt{sat}(\hat{u}_{k(\ell)}) = \mathtt{sign}(\hat{u}_{k(\ell)})\min(|\hat{u}_{k(\ell)}|, \bar{u}_{(\ell)}), \tag{2}$$

with $\bar{u}_{(\ell)} > 0$, $\ell \in \mathcal{I}[1, n_u]$, being the ℓ^{th} component of the symmetric saturation level $\bar{u}$. The vector of time-varying parameters ϑ_k, which are assumed measurable and available on-line (Briat, 2014), belongs to the unitary simplex defined by

$$\Theta = \left\{ \sum_{i=1}^{N} \vartheta_{k(i)} = 1,\ \vartheta_{k(i)} \geq 0,\ i \in \mathcal{I}[1, N] \right\}. \tag{3}$$

Thus, the matrices $A(\vartheta_k) \in \mathbb{R}^{n\times n}$ and $B(\vartheta_k) \in \mathbb{R}^{n\times n_u}$ can be written in a polytopic form, i.e. as a convex combination of N known vertices, as follows

$$[A(\vartheta_k)\ B(\vartheta_k)] = \sum_{i=1}^{N} \vartheta_{k(i)} [A_i\ B_i],\ \vartheta_k \in \Theta. \tag{4}$$

To stabilize the system (1), we adopt the following dynamic output-feedback controller:

$$\begin{aligned} x_{c,k+1} &= A_c(\vartheta_k)x_{c,k} + B_c(\vartheta_k)\hat{y}_k - E_c(\vartheta_k)\Psi(\hat{u}_k), \\ u_k &= C_c x_{c,k} + D_c\hat{y}_k, \end{aligned} \tag{5}$$

where $x_{c,k} \in \mathbb{R}^n$ is the control state, $\Psi(\hat{u}_k) : \mathbb{R}^{n_u} \to \mathbb{R}^{n_u}$ is the dead-zone non-linearity defined by $\Psi(\hat{u}_k) = \hat{u}_k - \mathtt{sat}(\hat{u}_k)$, and $\hat{y}_k$ is the most recently transmitted value of the measurable output y_k. To mitigate the effects caused by the saturating actuators (Tarbouriech et al., 2011), an anti-windup action, represented by the matrix $E_c(\vartheta_k) \in \mathbb{R}^{n\times n_u}$, is introduced on the controller structure. Therefore, it acts only when the saturation occurs, i.e., wherever $\Psi(\hat{u}_k) \neq \mathbf{0}$. The controller matrices (5) are supposed to have the following structure:

$$[A_c(\vartheta_k)\ B_c(\vartheta_k)\ E_c(\vartheta_k)] = \sum_{i=1}^{N} \vartheta_{k(i)} [A_{ci}\ B_{ci}\ E_{ci}].$$

Note that, as the matrices C_c and D_c do not depend on the parameter-varying ϑ_k, we have a partially parameter-dependent controller (PPD-DOF). Such controller differs from the one proposed by (de Souza et al., 2020), which has all matrices dependent on parameters. Moreover, in (de Souza et al., 2020), the matrices A_c and B_c have a quadratic dependence on the parameter ϑ_k, which leads to a more general polytopic representation. Also, observe that the controller must have the same dimension as the plant. To consider different orders, it is necessary to parameterize certain matrices, as is done in (de Souza et al., 2021).

To reduce the number of data exchange on sensor-to-controller and controller-to-actuator channels, we are employing two dependent event generators, which shares the same clock, as shown in Figure 1. In this case, the decision for output and control updates are periodically made according to the following rules, respectively,

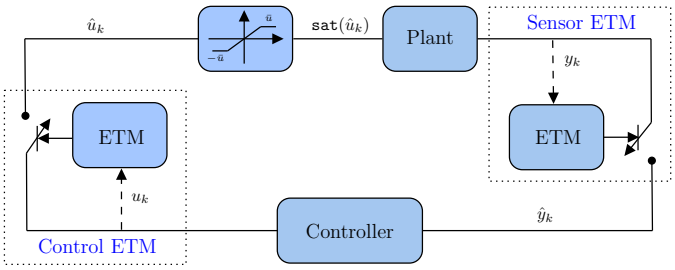

Figure 1. Event-triggering closed-loop system.

$$\hat{y}_k = \begin{cases} y_k, & \|\hat{y}_{k-1} - y_k\|^2_{Q_{\Delta y}} > \|y_k\|^2_{Q_y}, \\ \hat{y}_{k-1}, & \text{otherwise}, \end{cases} \tag{6}$$

and

$$\hat{u}_k = \begin{cases} u_k, & \|\hat{u}_{k-1} - u_k\|^2_{Q_{\Delta u}} > \|u_k\|^2_{Q_u}, \\ \hat{u}_{k-1}, & \text{otherwise}, \end{cases} \tag{7}$$

where the symmetric positive definite matrices $Q_{\Delta y}$, $Q_y \in \mathbb{R}^{n_y\times n_y}$ and $Q_{\Delta u}$, $Q_u \in \mathbb{R}^{n_u\times n_u}$ are triggering parameters to be designed. These matrices act as weights on the terms associated with the triggering conditions. Thus, their choice has a direct impact on the event-triggering policy, and, consequently, on the way to reduce the data transmission.

Due to the input saturation, the global stability is no longer guaranteed. In this case, the region of attraction

$\mathcal{R}_{\mathcal{A}}$, in the augmented space $\xi_k = \begin{bmatrix} x_k^\top & x_{c,k}^\top \end{bmatrix}^\top \in \mathbb{R}^{2n}$, must be considered. As the exact characterization of $\mathcal{R}_{\mathcal{A}}$ is, generally, a hard task, subsets with well-fitted representation, such as ellipsoidal and polyhedral sets, are determined. By denoting $\mathcal{R}_{\mathcal{E}}$ the estimated attraction region, then we are interested in computing $\mathcal{R}_{\mathcal{E}} \subseteq \mathcal{R}_{\mathcal{A}}$.

In the above context, we intend to solve the following problem.

Problem *1.* (Co-design). Given the saturated LPV system (1), co-design the PPD-DOF (5) and the two independent ETMs (6) and (7), ensuring the regional asymptotic stability of the closed-loop system, while reducing the transmission activity on the communication channels.

3. PRELIMINARIES RESULTS

The saturated LPV system (1) under the PPD-DOF (5), can be represented by the following model:

$$\begin{aligned} \xi_{k+1} &= \mathbb{A}(\vartheta_k)\xi_k - \mathbb{B}(\vartheta_k)\Psi(\hat{u}_k) + \mathbb{E}_y(\vartheta_k)e_{y,k} + \mathbb{E}_u(\vartheta_k)e_{u,k}, \\ u_k &= \mathbb{K}\xi_k + D_c e_{y,k}, \\ y_k &= \mathbb{C}\xi_k, \end{aligned} \tag{8}$$

where $e_{y,k} \in \mathbb{R}^{n_y}$ is the output error given by the difference between the latest transmission $\hat{y}_k$ and the latest sampling y_k, and $e_{u,k} \in \mathbb{R}^{n_u}$ is the control error given by the difference between the latest transmission $\hat{u}_k$ and the latest sampling u_k. The parameter-varying matrices assume the following structure:

$$[\mathbb{A}(\vartheta_k)\ \mathbb{B}(\vartheta_k)\ \mathbb{E}_u(\vartheta_k)\ \mathbb{E}_y(\vartheta_k)] = \sum_{i=1}^{N} \vartheta_{k(i)} [\mathbb{A}_i\ \mathbb{B}_i\ \mathbb{E}_{ui}\ \mathbb{E}_{yi}]$$

and are defined by

$$\mathbb{A}_i = \begin{bmatrix} A_i + B_i D_c C & B_i C_c \\ B_{ci} C & A_{ci} \end{bmatrix},\ \mathbb{B}_i = \begin{bmatrix} B_i \\ E_{ci} \end{bmatrix},\ \mathbb{E}_{ui} = \begin{bmatrix} B_i \\ \mathbf{0} \end{bmatrix},$$
$$\mathbb{E}_{yi} = \begin{bmatrix} B_i D_c \\ B_{ci} \end{bmatrix},\ \mathbb{K} = [D_c C\ C_c],\ \text{and}\ \mathbb{C} = [C\ \mathbf{0}].$$

Note that if y_k is updated at instant k, then from (6) it follows that $e_{y,k} = \hat{y}_k - y_k = y_k - y_k = \mathbf{0}$, and if y_k is not updated at instant k, then from (6) it also follows that $e_{y,k} = \hat{y}_k - y_k = \hat{y}_{k-1} - y_k$. Thus, the following inequality is always satisfied:

$$\|e_{y,k}\|^2_{Q_{\Delta y}} \leq \|y_k\|^2_{Q_y}. \tag{9}$$

In the same way, if u_k is updated at instant k, then from (7) we have that $e_{u,k} = u_k - u_k = \mathbf{0}$, and if u_k is not updated at instant k, then from (7) we have that $e_{u,k} = \hat{u}_{k-1} - u_k$. Consequently, the following condition always holds

$$\|e_{u,k}\|^2_{Q_{\Delta u}} \leq \|u_k\|^2_{Q_u}. \tag{10}$$

To investigate the regional asymptotic stability of the closed-loop system (8), we use the Lyapunov theory adopting the following candidate Lyapunov function

$$V(\xi_k) = \xi_k^\top P^{-1}(\vartheta_k)\xi_k, \tag{11}$$

where $P(\vartheta_k) = \sum_{i=1}^{N} \vartheta_{k(i)} P_i$, with $\mathbf{0} < P_i = P_i^\top \in \mathbb{R}^{2n \times 2n}$ and $\vartheta_k \in \Theta$. If (11) is a Lyapunov function, then the associated level set $\mathcal{L}_{\mathcal{V}}(1) = \{x_k \in \mathbb{R}^{2n} : V(x_k) \leq 1\}$, constitutes an estimate of the attraction region of the origin for the closed-loop system, i.e. $\mathcal{L}_{\mathcal{V}}(1) = \mathcal{R}_{\mathcal{E}}$. Due to the convexity of the formulation, $\mathcal{R}_{\mathcal{E}}$ can be computed as (Jungers and Castelan, 2011, Lemma 4) or (Figueiredo et al., 2021, Lemma 2, with $g = 1$):

$$\mathcal{R}_{\mathcal{E}} = \mathcal{L}_{\mathcal{V}}(1) = \bigcap_{\forall \vartheta_k \in \Theta} \mathcal{E}(P(\vartheta_k)^{-1}, 1) = \bigcap_{i \in \mathcal{I}[1,N]} \mathcal{E}(P_i^{-1}, 1), \tag{12}$$

with

$$\mathcal{E}(P_i^{-1}, 1) = \left\{\xi_k \in \mathbb{R}^{2n} : \xi_k^\top P_i^{-1} \xi_k \leq 1\right\}. \tag{13}$$

In addition, to handle the saturation effects, we use the following Lemma directly derived from (Tarbouriech et al., 2011, Lemma 1.6, p. 43).

Lemma 2. Let u_k given by (5), $\bar{u} \in \mathbb{R}^{n_u}_+$, and a matrix $\mathbb{G}(\vartheta_k) = \sum_{i=1}^{N} \vartheta_{k(i)} \mathbb{G}_i$ with $\mathbb{G}_i \in \mathbb{R}^{n_u \times 2n}$ for $\mathcal{I}[1, N]$ and $\vartheta_k \in \Theta$, such that

$$\mathcal{S}(\bar{u}) \triangleq \{\xi_k \in \mathbb{R}^{2n} : |\mathbb{G}(\vartheta_k)\xi_k| \leq \bar{u}\}.$$

If $\xi_k \in \mathcal{S}(\bar{u})$, then for any diagonal positive definite matrix $\mathbb{T} \in \mathbb{R}^{n_u \times n_u}$, the following inequality is verified

$$\Psi(\hat{u}_k)^\top \mathbb{T}(\Psi(\hat{u}_k) - (\mathbb{K} - \mathbb{G}(\vartheta_k))\xi_k - D_c e_{y,k} - e_{u,k}) \leq \mathbf{0}.$$

4. MAIN RESULTS

Let us start by introducing some matrices used in the development of the main conditions. Thus, inspired by Scherer et al. (1997), we consider the matrices X, Y, W and, $Z \in \mathbb{R}^{n \times n}$ to define

$$\mathbb{U} = \begin{bmatrix} X & \bullet \\ Z & \bullet \end{bmatrix},\quad \mathbb{U}^{-1} = \begin{bmatrix} Y & \bullet \\ W & \bullet \end{bmatrix}, \Phi = \begin{bmatrix} Y & \mathbf{I}_n \\ W & \mathbf{0} \end{bmatrix}, \tag{14}$$

which yield

$$\mathbb{U}\Phi = \begin{bmatrix} \mathbf{I}_n & X \\ \mathbf{0} & Z \end{bmatrix} \text{ and } \hat{\mathbb{U}} = \Phi^\top \mathbb{U} \Phi = \begin{bmatrix} Y^\top & M^\top \\ \mathbf{I}_n & X \end{bmatrix}, \tag{15}$$

where, by construction, we have

$$M^\top = Y^\top X + W^\top Z. \tag{16}$$

By partitioning matrix $P = \begin{bmatrix} P_{11} & \star \\ P_{21} & P_{22} \end{bmatrix}$, one obtains:

$$\hat{P}_i = \Phi^\top P_i \Phi = \begin{bmatrix} \hat{P}_{i11} & \star \\ \hat{P}_{i21} & \hat{P}_{i22} \end{bmatrix}, \tag{17}$$

with $\hat{P}_{i11} = Y^\top P_{i11} Y + W^\top P_{i12}^\top Y + Y^\top P_{i12} W + W^\top P_{i22} W$, $\hat{P}_{i21} = P_{i11}^\top Y + P_{i12} W$, and $\hat{P}_{i22} = P_{i11}$.

Theorem *3.* Consider there exist symmetric positive definite matrices $\hat{P}_i \in \mathbb{R}^{2n \times 2n}$, $Q_{\Delta u}$, $\hat{Q}_u \in \mathbb{R}^{n_u \times n_u}$, $Q_{\Delta y}$, $\hat{Q}_y \in \mathbb{R}^{n_y \times n_y}$, a positive definite diagonal matrix $S \in \mathbb{R}^{n_u \times n_u}$, and matrices X, Y, M, $\hat{A}_{ci}$, $\hat{B}_{ci}$, $\hat{C}_c$, $\hat{D}_c$, and $\hat{E}_{ci}$ of appropriate dimensions, and $H_i \in \mathbb{R}^{2n \times n_y}$, with $i \in \mathcal{I}[1, N]$, such that the following LMI conditions are feasible,

$$\begin{bmatrix} \hat{\mathbb{U}} + \hat{\mathbb{U}}^\top - \hat{P}_i & \star & \star & \star & \star & \star & \star \\ \mathbf{0} & Q_{\Delta u} & \star & \star & \star & \star & \star \\ \mathbf{0} & \mathbf{0} & Q_{\Delta y} & \star & \star & \star & \star \\ H_i - \Xi_{1ij} & -\mathbf{I}_{n_u} & -\hat{D}_c & 2S & \star & \star & \star \\ \Xi_{2i} & \Xi_{3i} & \Xi_{4i} & \Xi_{5i} & \hat{P}_j & \star & \star \\ \Xi_{1i} & \mathbf{0} & \hat{D}_c & \mathbf{0} & \mathbf{0} & \hat{Q}_u & \star \\ [C\ CX] & \mathbf{0} & \mathbf{0} & \mathbf{0} & \mathbf{0} & \mathbf{0} & \hat{Q}_y \end{bmatrix} > \mathbf{0}, \quad i \in \mathcal{I}[1, N] \tag{18}$$

and

$$\begin{bmatrix} \hat{\mathbb{U}} + \hat{\mathbb{U}}^\top - \hat{P}_i & \star \\ H_{i(\ell)} & \bar{u}^2_{(\ell)} \end{bmatrix} > \mathbf{0}, \quad i \in \mathcal{I}[1, N], \ell \in \mathcal{I}[1, n_u], \tag{19}$$

with

$$\Xi_{1i} = \begin{bmatrix}\hat{D}_c C & \hat{C}_c\end{bmatrix},\ \Xi_{3i} = \begin{bmatrix}Y^\top B_i \\ B_i\end{bmatrix},\ \Xi_{4i} = \begin{bmatrix}\hat{B}_{ci} \\ B_i\hat{D}_c\end{bmatrix},$$

$$\Xi_{2i} = \begin{bmatrix}Y^\top A_i + \hat{B}_{ci}C & \hat{A}_{ci} \\ A_i + B_i\hat{D}_c C & A_i X + B_i\hat{C}_c\end{bmatrix}$$

$$\Xi_{5i} = \begin{bmatrix}-\hat{E}_{ci} \\ -B_i S\end{bmatrix},\ \text{and}\ \hat{\mathbb{U}} = \begin{bmatrix}Y^\top & M^\top \\ \mathbf{I}_n & X\end{bmatrix}.$$

Then, by choosing non-singular matrices W and Z such that (16) holds, we have that the saturated LPV system (1) under the PPD-DOF (5) with matrices computed by

$$\begin{aligned}
D_c &= \hat{D}_c,\\
C_c &= (\hat{C}_c - D_c C X)Z^{-1},\\
B_{ci} &= (W^{-1})^\top(\hat{B}_{ci} - Y^\top B_i D_c),\\
A_{ci} &= (W^{-1})^\top(\hat{A}_{ci} - Y^\top(A_i + B_i D_c C)X - W^\top B_{ci} C X\\
&\quad - Y^\top B_i C_c Z)Z^{-1},\\
E_{ci} &= (W^{-1})^\top(\hat{E}_{ci} S^{-1} - Y^\top B_i),
\end{aligned} \tag{20}$$

subject to the ETMs (6) and (7) with matrices $Q_{\Delta u}$, $Q_u = \hat{Q}_u^{-1}$, $Q_{\Delta y}$ and $Q_y = \hat{Q}_y^{-1}$ is regionally asymptotically stable. Moreover, the region $\mathcal{R}_\mathcal{E}$, computed in (12)-(13), is an estimate of the region of attraction of the origin for the closed-loop system.

Proof. Fist of all, by supposing the feasibility of (18) and (19), from blocks (1,1), we have that $\hat{\mathbb{U}} + \hat{\mathbb{U}}^\top > 0$, and consequently, $\hat{\mathbb{U}}$ is non-singular. In view of (15), X and Y are also non-singular, and by rewritten $\hat{\mathbb{U}}$ as

$$\begin{bmatrix}Y^\top & M^\top \\ \mathbf{I}_n & X\end{bmatrix} = \begin{bmatrix}\mathbf{I}_n & Y^\top \\ \mathbf{0} & \mathbf{I}_n\end{bmatrix}\begin{bmatrix}\mathbf{0} & M^\top - Y^T X \\ \mathbf{I}_n & X\end{bmatrix}, \tag{21}$$

we can also verify the non-singularity of $(M^\top - Y^\top X)$. As a result, it is always possible to choose non-singular matrices W and Z, such that (16) is verified. This shows that the gains (20) are well-defined.

From now, we split the proof into two steps. In the first one, we show that any trajectory initialized in $\mathcal{L}_\mathcal{V}$ belongs to the polyhedral set $\mathcal{S}(\bar{u})$, which certifies the validity of Lemma 1. In the second, we prove the regional asymptotic stability of the closed-loop system.

Step 1: By considering the matrices (14)-(17), pre- and post-multiply (19) by the matrix $\texttt{diag}\{\Phi^{-\top}, 1\}$ and its transpose, respectively. Then, multiply the left-hand side of the resulting inequality by $\vartheta_{k(i)}$, sum it up for $i \in \mathcal{I}[1,N]$ and replace $H(\vartheta_k)$ by $G(\vartheta_k)\mathbb{U}\Phi$. After that, use the fact that $[P(\vartheta_k) - \mathbb{U}]^\top P^{-1}(\vartheta_k)[P(\vartheta_k) - \mathbb{U}] \geq \mathbf{0}$ to over-bound the block (1,1) by $\mathbb{U}^\top P^{-1}(\vartheta_k)U$. Then pre- and post-multiply the resulting inequality by the matrix $\texttt{diag}\{\mathbb{U}^{-\top}, 1\}$ to get

$$\begin{bmatrix}P^{-1}(\vartheta_k) & \star \\ \mathbb{G}(\vartheta_k)_{(\ell)} & \bar{u}^2_{(\ell)}\end{bmatrix} > \mathbf{0}. \tag{22}$$

Finally, apply Schur complement and pre- and post-multiply the resulting inequality by $\xi_k^\top$ and ξ_k, respectively, to obtain

$$-\xi_k^\top P(\vartheta_k)^{-1}\xi_k + \xi_k^\top \mathbb{G}(\vartheta_k)_{(\ell)}^\top(\bar{u}^2_{(\ell)})^{-1}\mathbb{G}(\vartheta_k)_{(\ell)}\xi_k \leq 0, \tag{23}$$

which ensures $V(\xi_k) = \xi_k^\top P^{-1}(\vartheta_k)x_k \leq 1$ and $|\mathbb{G}(\vartheta_k)\xi_k| \leq \bar{u}$, and, consequently, $\mathcal{R}_\mathcal{E} \subseteq \mathcal{S}(\bar{u})$. Therefore, any trajectory of the closed-loop system starting inside $\mathcal{R}_\mathcal{E}$ remains in $\mathcal{S}(\bar{u})$ and, consequently, Lemma 2 applies.

Step 2: By considering the change of variables $\hat{A}_{ci}$, $\hat{B}_{ci}$, $\hat{C}_c$, $\hat{D}_c$, and $\hat{E}_{ci}$, according to (20), and the matrices (14)-(17), pre- and post-multiply (18) by the matrix $\texttt{diag}\{\Phi^{-\top}, \mathbf{I}_{n_u}, \mathbf{I}_{n_y}, \Phi^{-\top}, \mathbf{I}_{n_u}, \mathbf{I}_{n_y}\}$ and its transpose, respectively. Then, multiply the left-hand side of the resulting inequality by $\vartheta_{k+1(j)}$ and $\vartheta_{k(i)}$, and sum it up for $i,j \in \mathcal{I}[1,N]$. After that, replace $H(\vartheta_k)$ by $\mathbb{G}(\vartheta_k)U$ and use the fact that $[P(\vartheta_k) - U]^\top P^{-1}(\vartheta_k)[P(\vartheta_k) - U] \geq \mathbf{0}$ or equivalently $U^\top + U - P(\vartheta_k) \leq U^\top P^{-1}(\vartheta_k)U$. Then, pre- and post-multiply the resulting inequality by the matrix $\texttt{diag}\{U^{-\top}, \mathbf{I}_{n_u}, \mathbf{I}_{n_y}, S^{-1}, \mathbf{I}_{2n}, \mathbf{I}_{n_u}, \mathbf{I}_{n_y}\}$ and its transpose, respectively, to obtain the inequality (24) (provided at the top of the next page). Next, apply Schur complement, pre- and post-multiply the resulting inequality by the augmented vector $\begin{bmatrix}\xi_k^\top & e_{u,k}^\top & e_{y,k}^\top & \Psi(\hat{u}_k)\end{bmatrix}^\top$ and its transpose, respectively, and replace $\mathbb{A}(\vartheta_k)\xi_k - \mathbb{B}(\vartheta_k)\Psi(\hat{u}_k) + \mathbb{E}_u(\vartheta_k)e_{u,k} + \mathbb{E}_y(\vartheta_k)e_{y,k}$ by ξ_{k+1} according to (8), to obtain

$$\begin{aligned}
&\xi_{k+1}^\top P^{-1}(\vartheta_{k+1})\xi_{k+1} - \xi_k^\top P^{-1}(\vartheta_k)\xi_k - 2\Psi(\hat{u}_k)^\top\mathbb{T}(\Psi(\hat{u}_k)\\
&\quad - (\mathbb{K} - \mathbb{G}(\vartheta_k))\xi_k - D_c e_{y,k} - e_{u,k}) - e_{u,k}^T Q_{\Delta u} e_{u,k}\\
&\quad + u_k^T Q_u u_k - e_{y,k}^T Q_{\Delta y} e_{y,k} + y_k^T Q_y y_k \leq 0
\end{aligned} \tag{25}$$

Finally, denote $S^{-1} = \mathbb{T}$, $\hat{Q}_y^{-1} = Q_y$, and $\hat{Q}_u^{-1} = Q_u$, and observe that $\xi_{k+1}^\top P^{-1}(\vartheta_{k+1})\xi_{k+1} - \xi_k^\top P^{-1}(\vartheta_k)\xi_k$ is equivalent to $V(\xi_{k+1}) - V(\xi_k) = \Delta V(\xi_k)$, to get

$$\begin{aligned}
\Delta V(\xi_k) &< 2\Psi(\hat{u}_k)^\top\mathbb{T}(\Psi(\hat{u}_k) - (\mathbb{K} - \mathbb{G}(\vartheta_k))\xi_k\\
&\quad - D_c e_{y,k} - e_{u,k}) < e_{u,k}^\top Q_{\Delta u} e_{u,k} - u_k^\top Q_u u_k\\
&\quad + e_{y,k}^\top Q_{\Delta y} e_{y,k} - y_k^\top Q_y y_k \leq 0.
\end{aligned}$$

Hence, the feasibility of (18) ensures the positivity of $V(\xi_k)$ given in (11) and the negativity of $\Delta V(\xi_k)$. Therefore, by Lyapunov theory, the regional stability of closed-loop system (8) subject to the ETMs (6) and (7) is ensured whenever the state trajectories evolve inside the estimated attraction region $\mathcal{R}_\mathcal{E}$, computed as in (12)-(13).

Note that Theorem 3 can be seen as a particular result of Theorem 2 proposed by (de Souza et al., 2020). An important aspect that distinguishes both conditions is their numerical complexity, which is associated with their number of variables ($\mathcal{K}$) and lines ($\mathcal{L}$). For Theorem 3, we have that $\mathcal{K}_1 = (5n + n_y + 3n_u)nN + 3n^2 + 3n_u^2 + 2n_y + (n + n_y)n_u$ and $\mathcal{L}_1 = (4n + 3n_u + 2n_y + (2n+1)n_u)N$. On the other hand, for Theorem 2 (de Souza et al., 2020), we have that $\mathcal{K}_2 = (4n + (n + n_y)((N + 1)/2) + 3n_u)nN + 3n^2 + 3n_u^2 + 2n_y + (n + n_y)n_u N$ and $\mathcal{L}_2 = ((4n + 3n_u + 2n_y)((N+1)/2) + (2n+1)n_u)N$. Note that the pair $(\mathcal{K}_2, \mathcal{L}_2)$ becomes higher than the pair $(\mathcal{K}_1, \mathcal{L}_1)$ as we increase the number of vertices (N). By admitting that the numerical complexity of the MATLAB solvers Lmilab and SeDumi are given respectively by: $\mathcal{K}^3\mathcal{L}$ and $\mathcal{K}^2\mathcal{L}^{2.5} + \mathcal{L}^{3.5}$ (Peaucelle et al., 2002), we plot in Figure 2 the ratio R_N between the numerical complexity of Theorem 2 (de Souza et al., 2020) and Theorem 3 for N varying from 1 up to 10. Since the ratios are bigger than 1 (except for N=1) for both solvers, we can conclude that the computation effort to design a FDP-DOF is bigger than to design a PPD-DOF.

$$\begin{bmatrix} P^{-1}(\vartheta_k) & \star & \star & \star & \star & \star & \star \\ \mathbf{0} & Q_{\Delta u} & \star & \star & \star & \star & \star \\ \mathbf{0} & \mathbf{0} & Q_{\Delta y} & \star & \star & \star & \star \\ -S^{-1}(\mathbb{K}-\mathbb{G}(\vartheta_k)) & -S^{-1} & -S^{-1}D_c & 2S^{-1} & \star & \star & \star \\ \mathbb{A}(\vartheta_k) & \mathbb{E}_u(\vartheta_k) & \mathbb{E}_y(\vartheta_k) & -\mathbb{B}(\vartheta_k) & P(\vartheta_{k+1}) & \star & \star \\ \mathbb{K} & \mathbf{0} & D_c & \mathbf{0} & \mathbf{0} & \hat{Q}_u & \star \\ \mathbb{C} & \mathbf{0} & \mathbf{0} & \mathbf{0} & \mathbf{0} & \mathbf{0} & \hat{Q}_y \end{bmatrix} > \mathbf{0}. \tag{24}$$

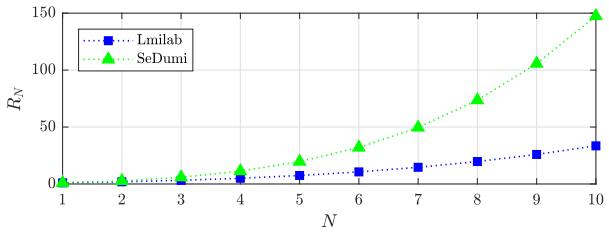

Figure 2. The ratio R_N between the numerical complexity of Theorem 2 (de Souza et al., 2020) and Theorem 3.

5. OPTIMIZATION PROCEDURE

The main objective here is to propose an optimization procedure that indirectly reduces the transmission activity on the network. By looking the event-triggering rules (6) and (7), we can see that they are a relative measure of the deviation between the latest transmission and the latest sampling of the output and control, respectively, with $Q_{\Delta y}$, $Q_{\Delta u}$, Q_y and Q_u acting as weighting on these measures. Thus, we have that the smaller the pair $(Q_{\Delta y}, Q_{\Delta u})$ and the larger the pair (Q_y, Q_u), the more the current output and control are allowed to deviate from their last transmission, and the fewer events are expected. In this sense, we propose the following optimization procedure

$$\mathcal{O}_1 : \begin{cases} \min & \mathtt{tr}(Q_{\Delta y} + \hat{Q}_y) + \mathtt{tr}(Q_{\Delta u} + \hat{Q}_u), \\ \text{subject to} & (18) \text{ and } (19). \end{cases} \tag{26}$$

Another objective of optimization consists in minimizing the transmission activity and in maximizing the estimate of the region of attraction at the same time. As minimizing only the transmission activity may result in a smaller estimate of the region of attraction, this optimization problem may be interesting to find a compromise between these two parameters. To maximize such a region, we can maximize the volume of an ellipsoidal $\mathcal{E}(R,1)$, defined as in (13), such that $\mathcal{E}(R,1) \subseteq \mathcal{E}(P(\vartheta_k)^{-1},1)$, which can be ensured by imposing $P_i^{-1} < R$ or still $\Phi^\top \hat{P}_i^{-1} \Phi < R$, for $i \in \mathcal{I}[1,N]$. However, the latter results in a non-convex LMI due to the presence of W in Φ. To overcome such an issue, let us consider only the part referring to the system states x_k, i.e.

$$\left[\begin{array}{c|c} R_1 & \star \\ \hline Y & \hat{P}_i \\ \mathbf{I}_n & \end{array}\right] > \mathbf{0}, \tag{27}$$

for $i \in \mathcal{I}[1,N]$, where R_1 consists of the first n rows and n columns of R. Thus, the following optimization procedure can reach such an objective

$$\mathcal{O}_2 : \begin{cases} \min & \mathtt{tr}(Q_{\Delta y} + \hat{Q}_y) + \mathtt{tr}(Q_{\Delta u} + \hat{Q}_u) + \mathtt{tr}(R), \\ \text{subject to} & (18), (19), \text{ and } (27). \end{cases} \tag{28}$$

It is interesting to highlight that, we can also avoid the problem of too small estimates of the region of attraction by having the specification of a region where stability must be guaranteed, as proposed in (Moreira et al., 2017).

6. NUMERICAL EXAMPLE

Consider the inverted pendulum system, which was also investigated in (de Souza et al., 2020)):

$$x_{k+1} = \begin{bmatrix} 1.0018 & 0.01 \\ 0.04\rho_k + 0.36 & 1.0018 \end{bmatrix} x_k + \begin{bmatrix} -0.001 \\ 0.025\rho_k - 0.184 \end{bmatrix} \mathtt{sat}(\hat{u}_k), \tag{29}$$

with $y_k = [1\ 0]\, x_k$, $\bar{u} = 1$ and $|\rho_k| \leq 1$. Our objective here is to made the co-design of the dynamic controller (5) and the two ETMs (6) and (7), so that both the transmission activity is as small as possible and the estimate of region of attraction is as bigger as possible. Thus, we solve the optimization procedure $\mathcal{O}_2$ given in (28) and obtain the ETM matrices $Q_{\Delta y} = 19.8744$, $Q_y = 0.1552$, $Q_{\Delta u} = 5.0260$ and $Q_u = 0.0392$ and the following dynamic controller matrices

$$A_{c1} = \begin{bmatrix} 0.3275 & -2.1957 \\ -0.0783 & -0.5247 \end{bmatrix},\ B_{c2} = \begin{bmatrix} -2.1265 \\ 0.5082 \end{bmatrix},$$
$$A_{c2} = \begin{bmatrix} 0.1300 & -3.2109 \\ -0.0315 & 0.7657 \end{bmatrix},\ B_{c1} = \begin{bmatrix} -4.8104 \\ 1.1502 \end{bmatrix},$$
$$C_c = [-0.3260\ \ -1.8837],\ \text{and}\ D_c = 5.9883.$$

From that, we simulate the closed-loop response of the system by considering the initial conditions $x_0 = [-0.1903\ \ -0.4216]$ and $x_{c,0} = [0\ 0]$, which are inside the estimate of the region of attraction. Figure 4 shows the states, the control input, and the parameter-varying, where we can see the asymptotic stability of the system despite the saturation in the first instants of the simulation. On the other hand, Figure 3 presents the inter-events time of the sensor and the controller. Note that the events that occur asynchronously in the sensor and in the controller are marked with '○' and '○', respectively, and synchronous with '○'. In this case, the update rate of the output and the control signals was 47.67% and 56.33%, respectively, thus, saving a significant amount of samples to be transmitted.

Furthermore, we are also interested in comparing the results obtained using the partially parameter-dependent (PPD) and the full parameter-dependent (FPD) dynamic controller, which is proposed in (de Souza et al., 2020). For this purpose, we solve the optimization problem $\mathcal{O}_2$ given in (28) with Theorem 2 in (de Souza et al., 2020) and achieve the ETM matrices $Q_{\Delta y} = 19.8541$, $Q_y = 0.1566$, $Q_{\Delta u} = 5.0174$ and $Q_u = 0.0393$. From that, we simulate the closed-loop response considering the same initial conditions for the plant and controller. In such a

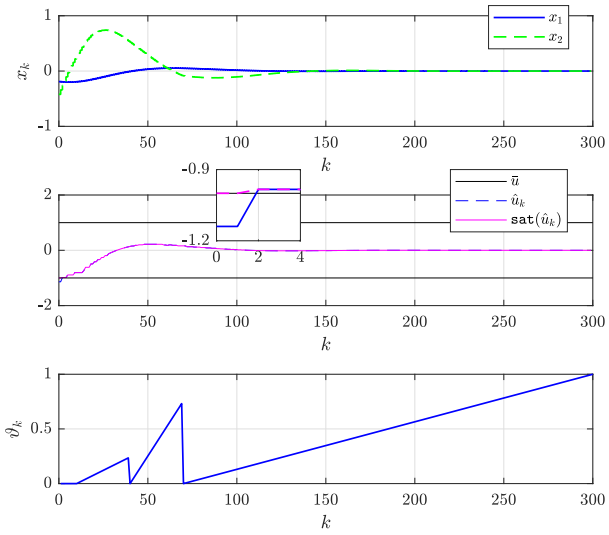

Figure 3. The closed-loop system response.

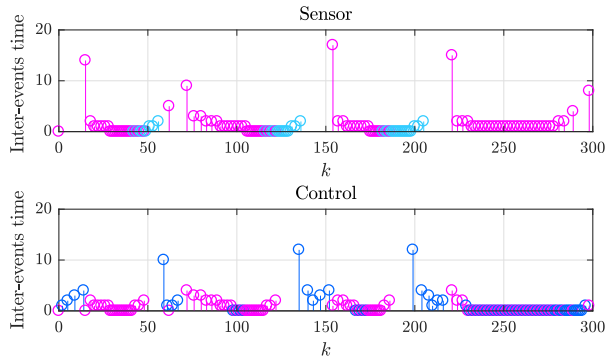

Figure 4. Inter-events time of the sensor and controller.

case, the update rate of the output and the control signals were 50% and 45%, respectively. Thus, we have that the transmission activity using the PPD-DOF is 9% (total) greater than using the FPD-DOF, which is expected since the FDP-DOF design is more general. In addition, we plot the estimate of the region of attraction for both cases, as shown in Figure 5. Although the PPD-DOF achieved a slightly worse result in terms of transmission activity (total), observe that its estimate of the region of attraction ($\mathcal{R}_\mathcal{E}$) comprises more initial conditions than the one of the FPD-DOF. Furthermore, it is important to re-emphasize that the computational effort to design a PPD-DOF is less than to design a FDP-DOF, since the LMI-conditions are simpler. Also, the simpler structure of a PPD-DOF leads to a less complex implementation (Klug and Castelan, 2012). Therefore, as we can see, there are pros and cons to implement both controllers. It is the design specifications that will determine the most appropriate one.

7. CONCLUSION

This paper examines the event-triggered control design problem for discrete LPV systems subject to saturating actuators. Differently from (de Souza et al., 2020), the

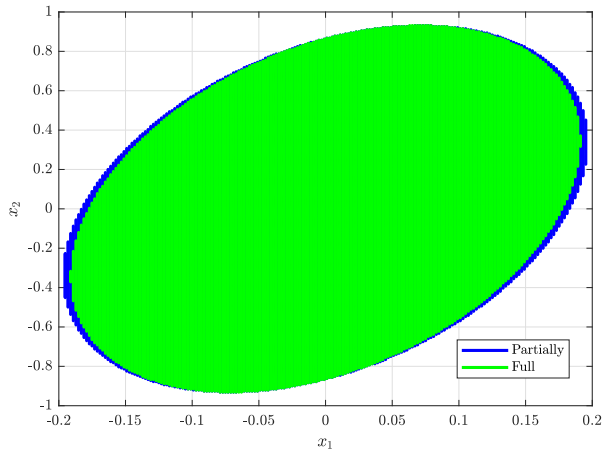

Figure 5. $\mathcal{R}_\mathcal{E}$ for the partially (−) and full (−) parameter-dependent dynamic controller.

proposed controller is partially dependent on the time-varying parameters (PPD-DOF), simplifying the controller implementation. The output signal and control input are sent through the communication network based on two independent event-triggering schemes that shares the same clock. Convex conditions ensure the regional asymptotic stability of the closed-loop system for every initial condition belonging to the estimate of the region of attraction. Optimization procedures are derived allowing to minimize the data update rate and optionally to maximize the domain of attraction at the same time. A numerical example is used to illustrate and compare the achievements obtained using the PPD-DOF and the FPD-DOF (proposed in (de Souza et al., 2020)), pointing out the pros and cons of each design.

REFERENCES

Abdelrahim, M., Postoyan, R., Daafouz, J., and Nešić, D. (2015). Stabilization of nonlinear systems using event-triggered output feedback controllers. *IEEE transactions on automatic control*, 61(9), 2682–2687.

Braga, M.F., Morais, C.F., Oliveira, E.S.T.R., and P.L.D.Peres (2015). Discretization and event triggered digital output feedback control of LPV systems. *Systems & Control Letters*, 86, 54–65.

Briat, C. (2021). Stability analysis and stabilization of LPV systems with jumps and (piecewise) differentiable parameters using continuous and sampled-data controllers. *Nonlinear Analysis: Hybrid Systems*, 41, 101040.

Briat, C. (2014). *Linear Parameter-Varying and Time-Delay Systems: Analysis, Observation, Filtering & Control*. Berlin.

Caigny, J.D., Camino, J.F., Oliveira, R., Peres, P., and Swevers, J. (2012). Gain-scheduled dynamic output feedback control for discrete-time lpv systems. *International Journal of Robust and Nonlinear Control*, 22(5), 535–558.

de Souza, C., Castelan, E., and Leite, V. (2021). Dynamic controllers for local input-to-state stabilization of discrete-time linear parameter-varying systems with delay and saturating actuators. *International Journal of Robust and Nonlinear Control*, 31(1), 131–147.

de Souza, C., Leite, V., Tarbouriech, S., and Castelan, E. (2020). Event-triggered policy for DOF stabilization of discrete-time LPV systems under input constraints. *System & Control Letters*, 153, 104950.

Ding, S., Xie, X., and Liu, Y. (2020). Event-triggered static/dynamic feedback control for discrete-time linear systems. *Information Sciences*.

Figueiredo, L.S., Lacerda, M.J., and Leite, V.J.S. (2021). Design of saturating state feedback control laws for discrete-time linear parameter varying systems through homogeneous polynomial parameter-dependent functions. *International Journal of Robust and Nonlinear Control*, 31(14), 6585–6601.

Girard, A. (2014). Dynamic triggering mechanisms for event-triggered control. *IEEE Transactions on Automatic Control*, 60(7), 1992–1997.

Golabi, A., Meskin, N., Tóth, R., Mohammadpour, J., and Donkers, T. (2016). Event-triggered control for discrete-time linear parameter-varying systems. In *2016 American Control Conference (ACC)*, 3680–3685.

Golabi, A., Meskin, N., Tóth, R., Mohammadpour, J., Donkers, T., and Davoodi, M. (2017). Event-triggered constant reference tracking control for discrete-time LPV systems with application to a laboratory tank system. *IET Control Theory & Applications*, 11(16), 2680–2687.

Heemels, W., Donkers, M., and Teel, A. (2012). Periodic event-triggered control for linear systems. *IEEE Transactions on Automatic Control*, 58(4), 847–861.

Huang, J.J., Pan, X.Z., and Hao, X.Z. (2020). Event-triggered and self-triggered $\mathcal{H}_\infty$ output tracking control for discrete-time linear parameter-varying systems with network-induced delays. *International Journal of Systems Science*, 1–20.

Jungers, M. and Castelan, E.B. (2011). Gain-scheduled output control design for a class of discrete-time nonlinear systems with saturating actuators. *Systems & Control Letters*, 60(3), 169–173.

Klug, M. and Castelan, E.B. (2012). Compensadores dinâmicos para sistemas discretos no tempo com parametros variantes e aplicação a um sistema fuzzy takagi-sugeno. *Sba: Controle & Automação Sociedade Brasileira de Automatica*, 23(5), 517–529.

Moreira, L.G., Groff, L.B., Gomes da Silva Jr, J.M., and Coutinho, D. (2017). Event-triggered control for nonlinear rational systems. *IFAC-PapersOnLine*, 50(1), 15307–15312.

Peaucelle, D., Didier, H., Labit, Y., and Taitz, K. (2002). User's guide for SEDUMI INTERFACE 1.04.

Scherer, C., Gahinet, P., and Chilali, M. (1997). Multiobjective output-feedback control via LMI optimization. *IEEE Transactions on automatic control*, 42(7), 896–911.

Shamma, J.S. (2012). An overview of LPV systems. In *Control of linear parameter varying systems with applications*, 3–26. Springer.

Shen, Y., Li, F., Zhang, D., Wang, Y.W., and Liu, Y. (2019). Event-triggered output feedback $\mathcal{H}_\infty$ control for networked control systems. *International Journal of Robust and Nonlinear Control*, 29(1), 166–179.

Tabuada, P. (2007). Event-triggered real-time scheduling of stabilizing control tasks. *IEEE Transactions on Automatic Control*, 52(9), 1680–1685.

Tarbouriech, S., Garcia, G., Gomes da Silva Jr., J.M., and Queinnec, I. (2011). *Stability And Stabilization Of Linear Systems With Saturating Actuators*. Springer.

Wu, W., Reimann, S., and Liu, S. (2014). Event-triggered control for linear systems subject to actuator saturation. *IFAC Proceedings Volumes*, 47(3), 9492–9497.

Xie, X., Li, S., and Xu, B. (2018). Output-based event-triggered control for networked control systems: tradeoffs between resource utilisation and robustness. *IET Control Theory & Applications*, 12(15), 2138–2147.

Zuo, Z., Li, Q., Li, H., and Wang, Y. (2016). Co-design of event-triggered control for discrete-time systems with actuator saturation. In *2016 12th World Congress on Intelligent Control and Automation (WCICA)*, 170–175. IEEE.